Supplementary materials

As a supplement to the main document of *Freak Wave in a Two-Dimensional Directional Wavefield with Bottom Topography Change: Part I. Normal Incident Wave*, this section aims to give details of the numerical model and how we decide the calculation conditions and optimistic output interval.

To satisfy the zero-mean SSS process of a 2D wavefield, we need to give the optimistic sampling distance $\mathrm{d}y$ and lateral computational domain L_y for better accuracy and computational efficiency. In **Figure S1** and **Figure S2**, we give the kurtosis μ_4 and skewness μ_3 from a single sample starting from the same condition at different resolution at BFI = 0.4, σ_θ = 0.3, and water depth kh = 5. μ_4 and μ_3 in the 2D wavefield is gained from the surface elevation at a fixed point in time series. We consider 8 kinds of lateral resolution from (a) ~ (h): $\mathrm{d}y$ = 0.0057L_0, 0.017L_0, 0.028L_0, 0.057L_0, 0.143L_0, 0.28L_0, 0.85L_0, 1.43L_0, and output the longitudinal result in the same resolution with the lateral. Based on the degree of keeping main information, we get an approximate range of optimistic $\mathrm{d}y$ around 0.3L_0.

In **Figure S3**, we give the normalized auto-correlation coefficient of the surface elevation η at t = 40T_0 in the sequence of y on different spatial step x = 10L_0, 20L_0, 30L_0 with different L_y and $\mathrm{d}y$. At y = 0, the auto-correlation coefficient is 1 since it's totally related to itself. As the calculation moves from x = 10L_0 to 30L_0 on the propagation direction, the difference caused by different $\mathrm{d}y$ gradually accumulates in the result from L_y = 10L_0 and 20L_0. In the L_y = 30L_0, the auto-correlation curve is basically under 0.5, and the result for different $\mathrm{d}y$ is almost the same, which implies L_y = 30L_0 is long enough in the simulation. In **Figure S4**, we give the normalized cross-correlation coefficient of the surface elevation η in different sequences at different $\mathrm{d}y$ with L_y = 30L_0. Three columns on the left are in time series, and we select $\eta(t)$ at $y = 0$ as the first sequence and $\eta(t)$ at $y = D_y$ as the other sequence at x = 0, 20L_0, 30L_0 to give their normalized cross-correlation. The first column from the right is in spatial series, and we select $\eta(x)$ at $y = 0$ as the first sequence and $\eta(x)$ at $y = D_y$ as the other sequence at t = 40T_0 to give their normalized cross-correlation. The results are basically lower than 0.25, which means the correlation between the two sequences is weak enough. To make the calculation efficient, we choose $L_y = 30L_0$ and $d_y = 0.5L_0$ in Monte Carlo simulation.

After finishing the initial setting of the computing environment, we examine the convergence of the Monte Carlo simulation. We take the kurtosis μ_4 of surface elevation η as the index and give the average μ_4 of a 2D wavefield from different ensemble sizes M. In **Figure S5**, we give the spatial evolution of μ_4 from different ensemble size M at a 2D flat bottom with kh = 5, initial BFI = 0.4 and σ_θ = 0.5. The result shows, μ_4 is closed to be convergent when $M \geq$ 200, and the improvement from enlarging M is not obvious when $M \geq$ 300. In **Figure S6**, we give the variation of mean value and standard deviation of μ_4 with ensemble size M at (x, y) = $(20L_0, 15L_0)$ with kh = 5, initial BFI = 0.4 and σ_θ = 0.5. When $M \geq$ 200, the mean value and standard deviation both become convergent enough. Corresponding results in 2D are given in **Figure S7**. In a 2D area, a totally convergent mean value of μ_4 requires a very large ensemble size M, but we think the approximate range of the distribution of μ_4 in $M \geq$ 300 is enough for the following discussion. Therefore, the ensemble size M in Monte Carlo result and statistical analysis in the following part is 300.

Figure S8 gives the original data of the fit curves through the tenth-order polynomial in **Figure 8** in main document as a reference.

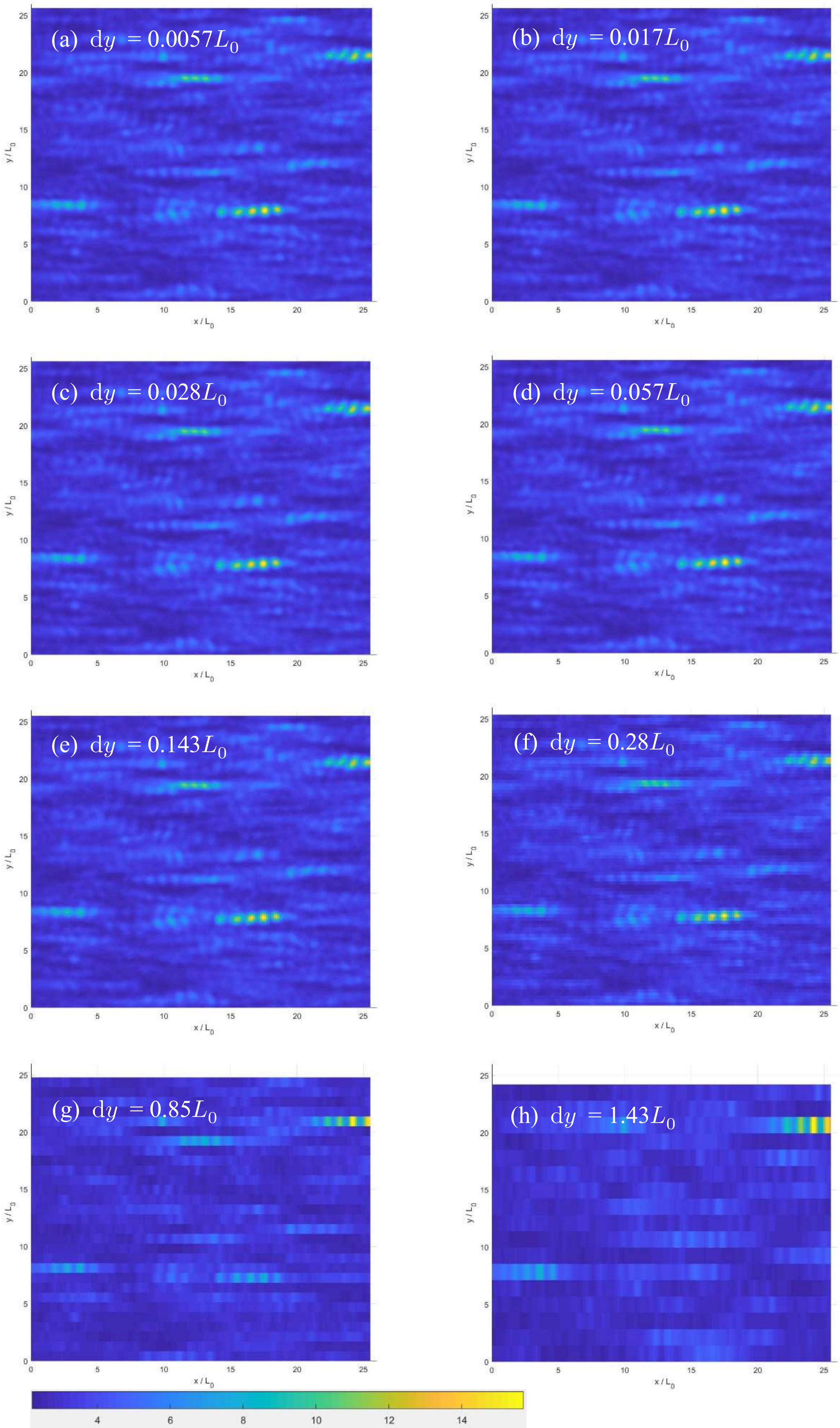

Figure S1 μ_4 from the same sample at different resolution at BFI = 0.4, σ_θ = 0.3, kh =5

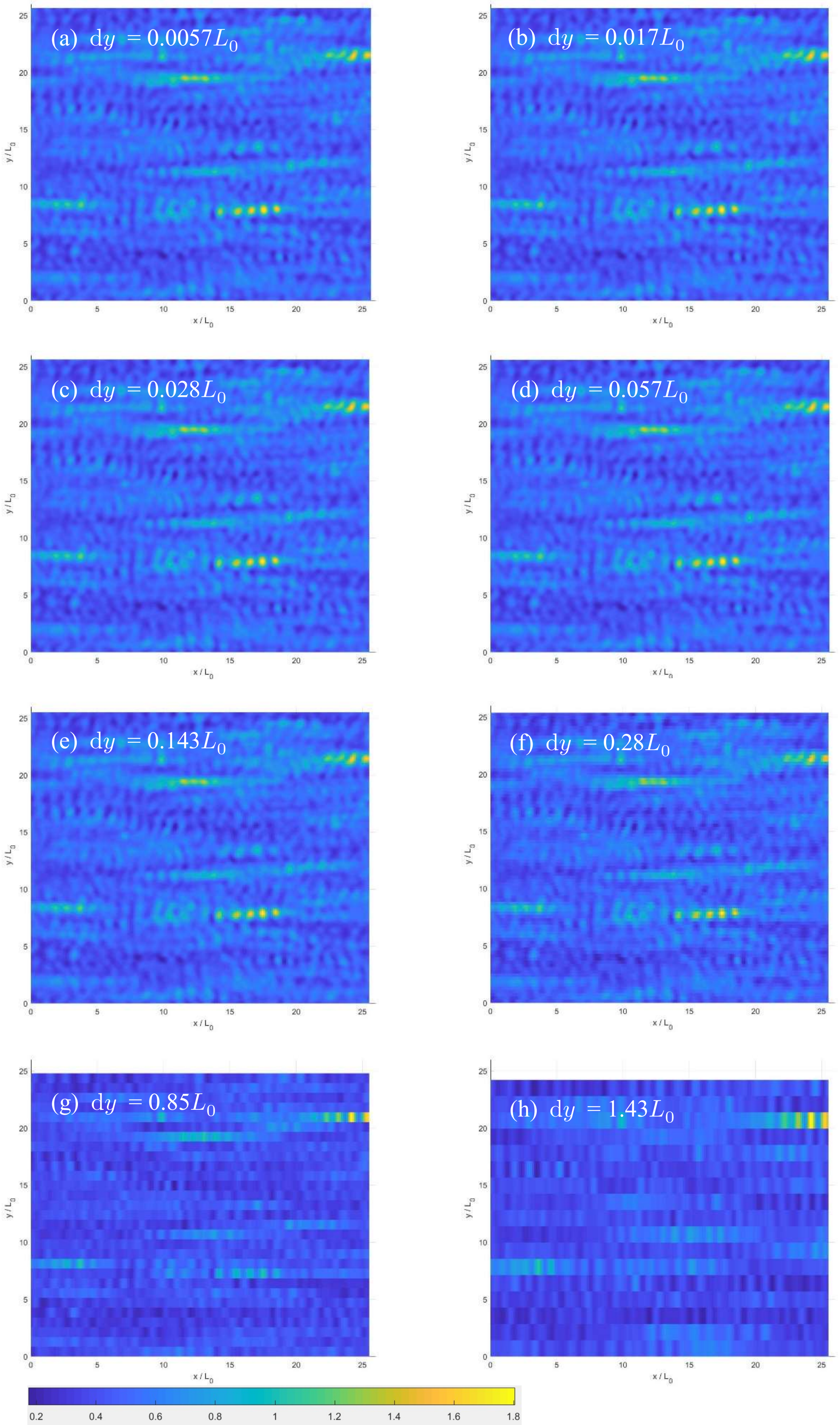

Figure S2 μ_3 from the same sample at different resolution at BFI = 0.4,σ_θ = 0.3, kh = 5

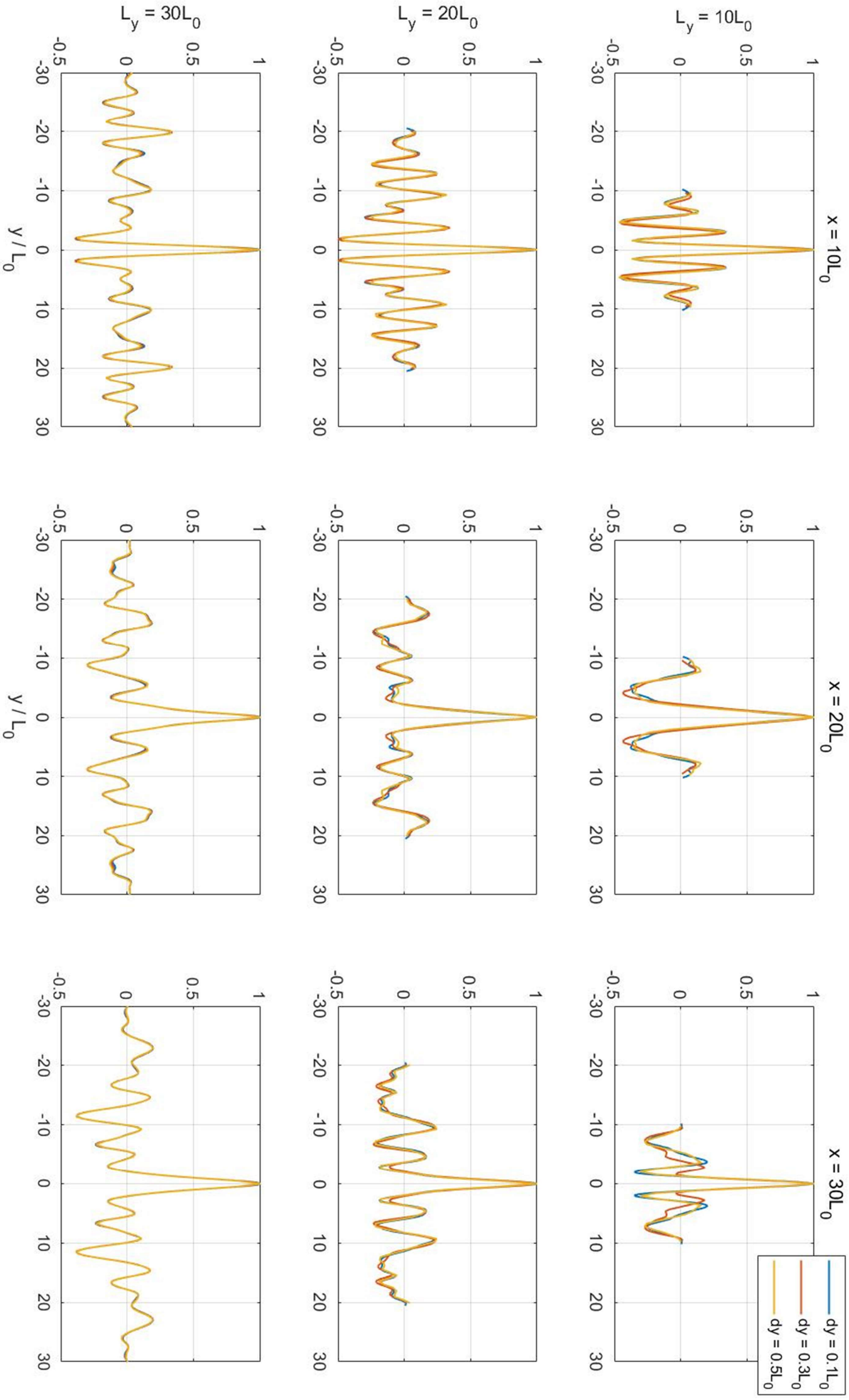

Figure S3 Normalized auto-correlation of the surface elevation in the sequence of y on different spatial step with different model setting at $t = 40T_0$

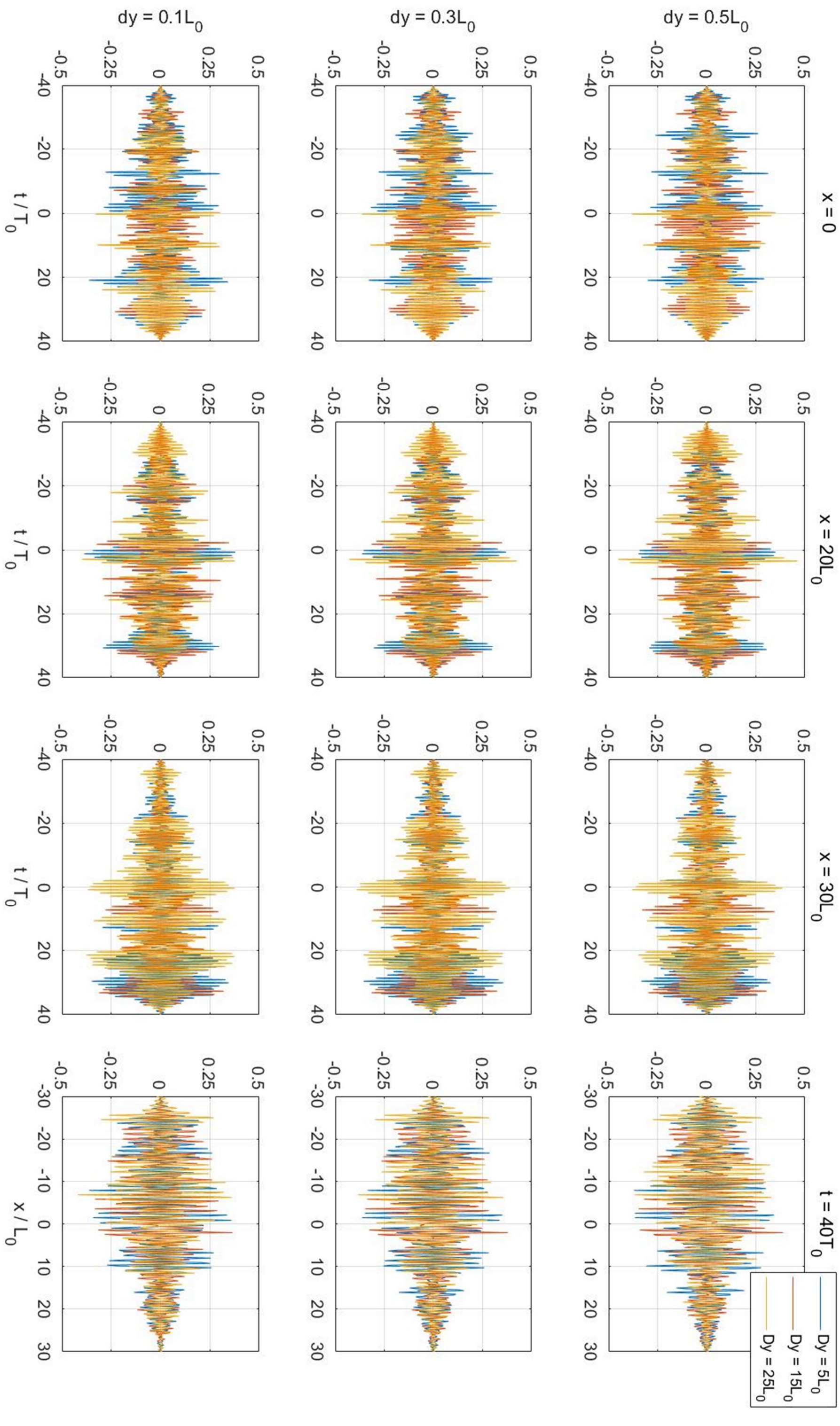

Figure S4 Normalized cross-correlation between surface elevation at $y = 0$ and $y = D_y$ in time and spatial series at different sections with different model setting

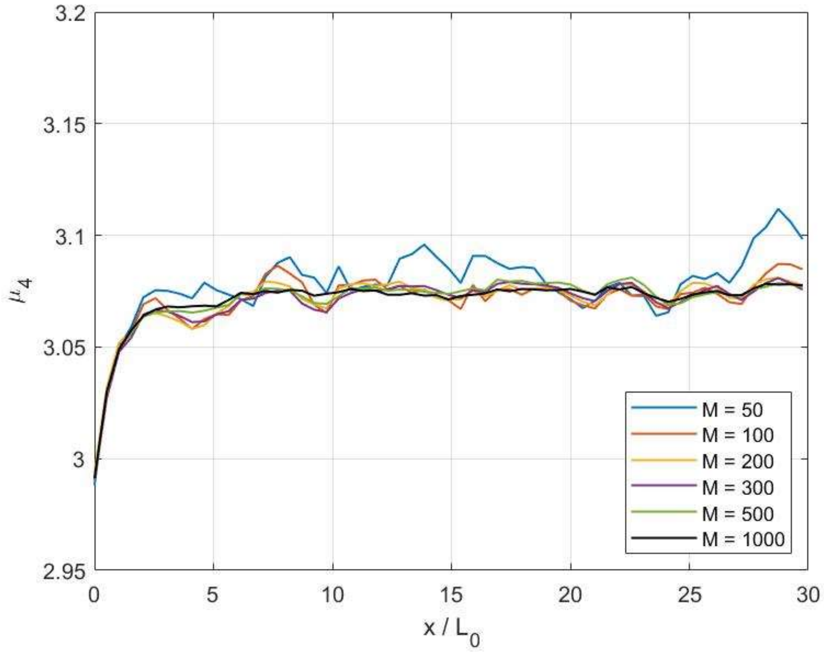

Figure S5 Spatial evolution of kurtosis of surface elevation from different ensemble size M at a 2D flat bottom with kh = 5, initial BFI = 0.4 and σ_θ = 0.5

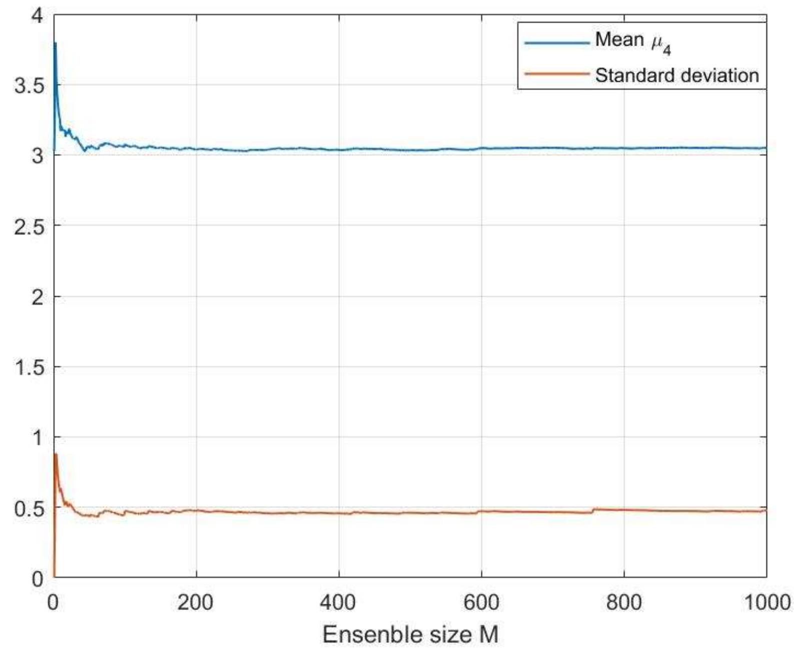

Figure S6 Variation of mean value and standard deviation of kurtosis with ensemble size M at (x, y) = ($20L_0$, $15L_0$) with kh = 5, initial BFI = 0.4 and σ_θ = 0.5

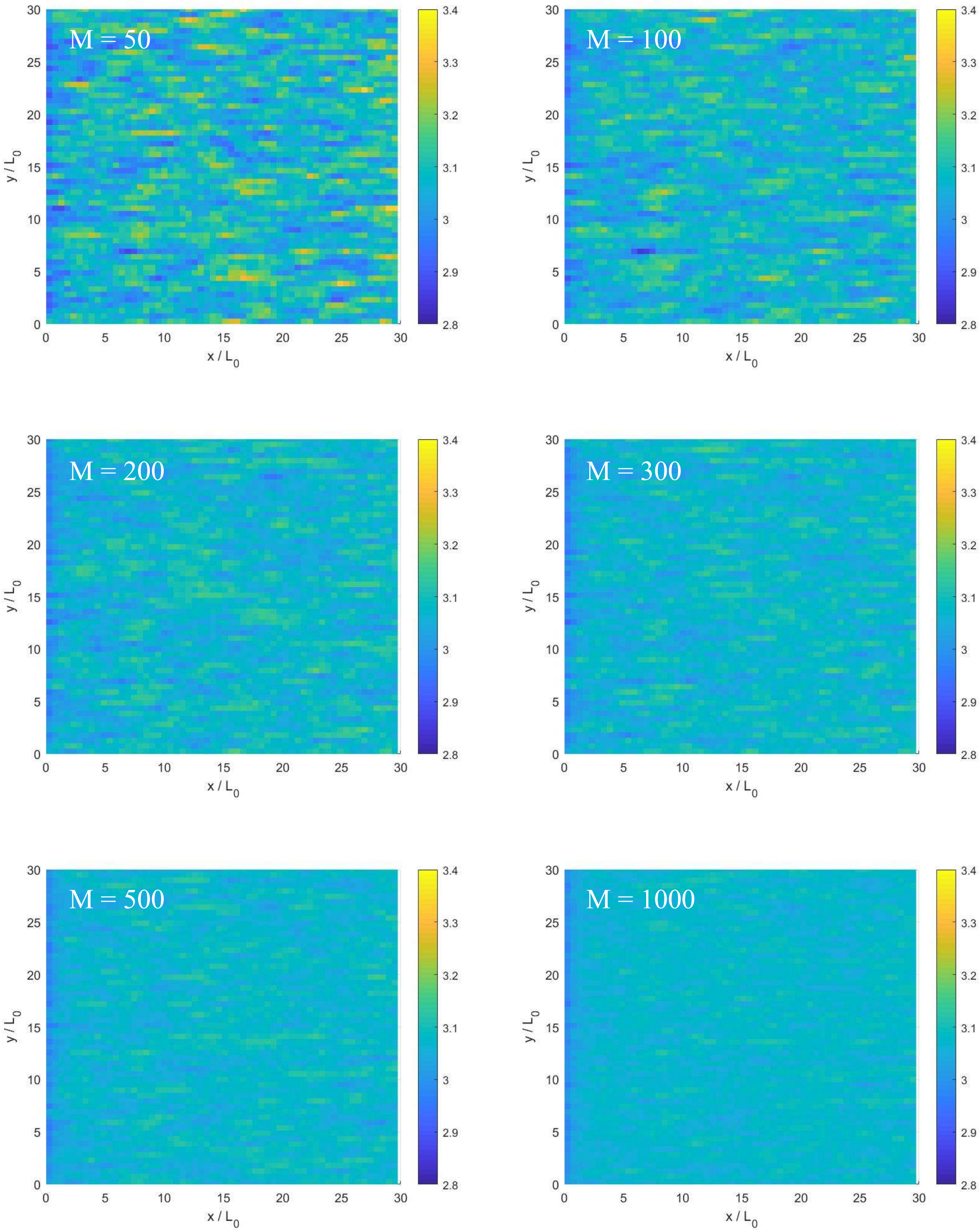

Figure S7 μ_4 of surface elevation from different ensemble size M at a 2D flat bottom with kh = 5, initial BFI = 0.4 and σ_θ = 0.5

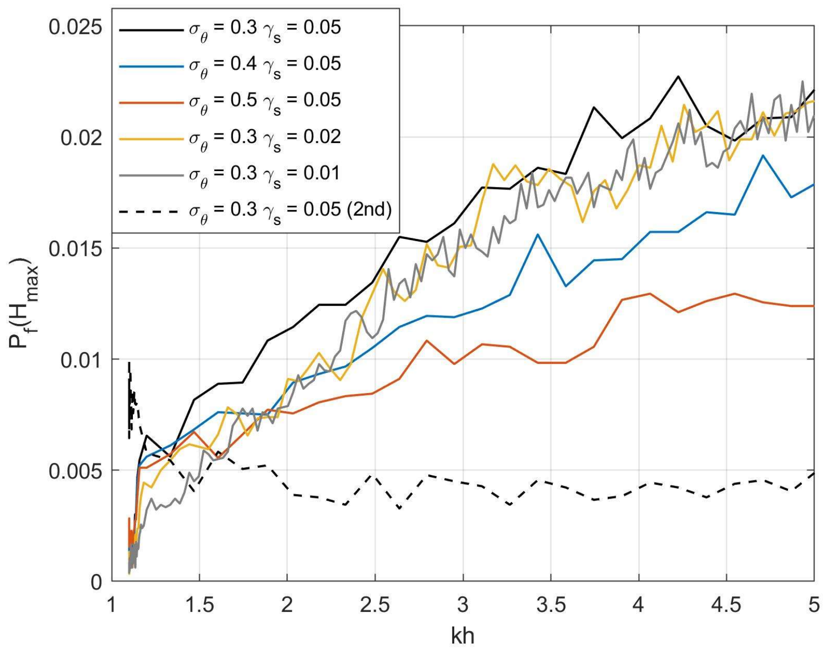

(a) probability of $H_{\max} > 8\eta_{\mathrm{rms}}$

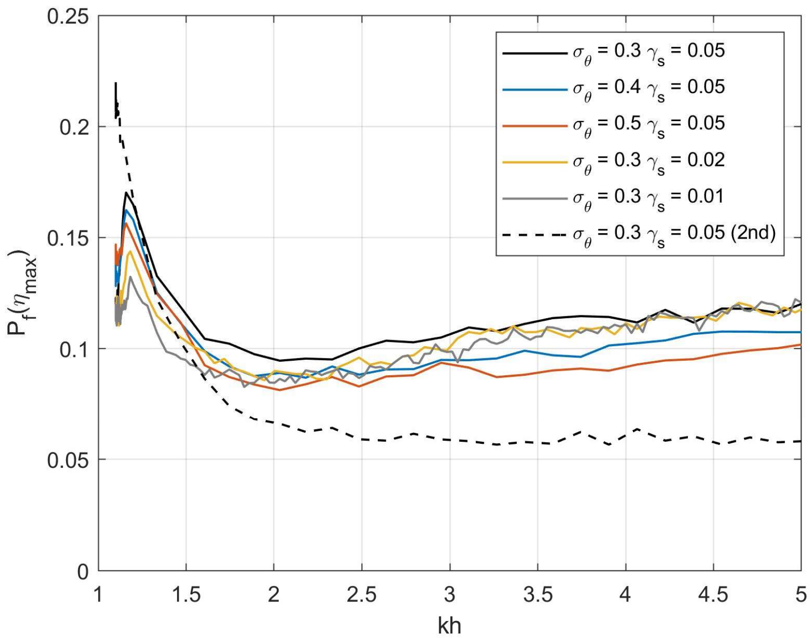

(b) probability of $\eta_{\max} > 4\eta_{\mathrm{rms}}$

Figure S8 Occurrence probability of the freak wave in wave height and free surface elevation distribution at initial BFI = 0.4 from different σ_θ and γ_s